Mon. Not. R. Astron. Soc. **000**, 1–?? (2002) Printed 2 June 2016 (MN LATEX style file v2.2)

A Revised Analysis of Gamma Ray Bursts' prompt efficiencies

Paz Beniamini ⋆, Lara Nava and Tsvi Piran
Racah Institute for Physics, The Hebrew University, Jerusalem, 91904, Israel

arXiv:1606.00311v1 [astro-ph.HE] 1 Jun 2016

Accepted ... Received ...; in original form ...

ABSTRACT

The prompt Gamma-Ray Bursts' (GRBs) efficiency is an important clue on the emission mechanism producing the γ-rays. Previous estimates of the kinetic energy of the blast waves, based on the X-ray afterglow luminosity L_X, suggested that this efficiency is large, with values above 90% in some cases. This poses a problem to emission mechanisms and in particular to the internal shocks model. These estimates are based, however, on the assumption that the X-ray emitting electrons are fast cooling and that their Inverse Compton (IC) losses are negligible. The observed correlations between L_X (and hence the blast wave energy) and $E_{\gamma,\rm iso}$, the isotropic equivalent energy in the prompt emission, has been considered as observational evidence supporting this analysis. It is reasonable that the prompt gamma-ray energy and the blast wave kinetic energy are correlated and the observed correlation corroborates, therefore, the notion L_X is indeed a valid proxy for the latter. Recent findings suggest that the magnetic field in the afterglow shocks is significantly weaker than was earlier thought and its equipartition fraction, ϵ_B, could be as low as 10^{-4} or even lower. Motivated by these findings we reconsider the problem, taking now IC cooling into account. We find that the observed $L_X - E_{\gamma,\rm iso}$ correlation is recovered also when IC losses are significant. For small ϵ_B values the blast wave must be more energetic and we find that the corresponding prompt efficiency is significantly smaller than previously thought. For example, for $\epsilon_B \sim 10^{-4}$ we infer a typical prompt efficiency of $\sim 15\%$.

Key words: gamma-ray burst: general

1 INTRODUCTION

Gamma-Ray Bursts (GRBs) are extremely energetic pulses of γ-rays, associated with a relativistic jet launched following the core collapse of a massive star or a compact binary merger. Energy dissipation internal to the jet is thought to be responsible for the emission of the prompt γ-rays, while the subsequent collision between the jet and the external environment produces the longer-lived afterglow.

Two critical quantities in this model are the energy radiated in the first prompt phase, and the energy that remains in the blast-wave and that powers the afterglow. While the first can be directly estimated from prompt observations, the latter can be inferred only indirectly from afterglow observations. The sum gives the total amount of initial explosion energy, an important information that constrains the nature of the progenitor. The ratio indicates the efficiency of the prompt phase (i.e. the efficiency of the dissipation mechanism times the efficiency of the radiative process).

In models involving hydrodynamic jets, large dissipation efficiencies are unlikely realized: maximal values are estimated to be $\lesssim 0.2$ (Kobayashi et al. 1997; Daigne & Mochkovitch 1998; Lazzati et al. 1999; Kumar 1999; Beloborodov 2000; Guetta et al. 2001; Beniamini & Piran 2013; Vurm et al. 2013). In electromagnetic jets, it may be possible to obtain higher dissipative efficiencies (see e.g. Zhang & Yan 2011). However the situation is much less certain (see e.g. Granot et al. 2015; Kumar & Crumley 2015; Beniamini & Granot 2016). The efficiency is unlikely to approach unity: magnetic field lines approaching the reconnection zone are unlikely to be exactly anti-parallel, and a significant portion of the EM energy could remain undissipated. Furthermore, a major challenge in models that rely on synchrotron to produce the prompt radiation is to explain the observed spectral indices below the sub-MeV peak. This may be viable if the electrons are only "marginally fast cooling" or if their spectra is modified by IC cooling. Both possibilities suggest that the efficiency of radiation is only moderate (Derishev et al. 2001; Bošnjak et al. 2009; Daigne 2011; Beniamini & Piran 2013, 2014). Determining

⋆ E-mail:paz.beniamini@gmail.com

the overall efficiency would therefore give important clues on the still uncertain nature of the mechanism responsible for the prompt radiation. It follows that inferring reliable estimates of the (isotropically equivalent) kinetic energy $E_{\rm kin}$ that remains in the blast wave after the prompt phase is of paramount importance.

Under certain conditions, $E_{\rm kin}$ can be quite firmly estimated from afterglow observations. If observations are performed at a frequency where the emission is dominated by fast cooling electrons (i.e. a frequency larger than the characteristic synchrotron frequencies) *and* if these electrons do not suffer from significant Inverse Compton (IC) losses, then the afterglow luminosity at such a frequency provides a robust estimate of the energy stored in the accelerated electrons, which is in turn directly related to the kinetic energy of the blast wave (Kumar 2000; Freedman & Waxman 2001).

It has been argued that electrons emitting X-ray afterglow radiation fulfil these conditions. A correlation between the (isotropically equivalent) X-ray luminosity L_X and the (isotropically equivalent) energy released during the prompt phase $E_{\gamma,\rm iso}$ has indeed been observed in both long and short GRBs. This supported the notion that the X-ray luminosity is a good proxy for the kinetic energy, and hence it must be produced by fast cooling electrons that undergo negligible IC losses. Under this assumption, several studies have exploited X-ray observations to estimate the energies of GRB blast waves and eventually also the prompt efficiencies ϵ_γ (Freedman & Waxman 2001; Berger et al. 2003; Lloyd-Ronning & Zhang 2004; Berger 2007; Nysewander et al. 2009; D'Avanzo et al. 2012; Wygoda et al. 2015). Most of these studies inferred relatively low kinetic energies that correspond to large prompt efficiencies $\epsilon_\gamma = E_{\gamma,\rm iso}/(E_{\gamma,\rm iso}+E_{\rm kin})$. Values larger than 50% and up to more than 90% have been estimated in some cases (Granot et al. 2006; Ioka et al. 2006; Nousek et al. 2006; Zhang et al. 2007). The discovery of X-ray plateaus in many X-ray light-curves has increased the severity of the efficiency problem and poses even more serious challenge for the internal shocks model.

Recently, the location of the cooling frequency compared to the X-ray frequency and the relevance of IC losses have been brought into question. In a study involving bursts with temporally extended GeV emission, Beniamini et al. (2015) have shown (with multi wavelength modelling performed under the assumption that GeV radiation originated at the external shocks) that X-ray emitting electrons are either slow cooling or they suffer from significant IC losses, making the X-ray flux not directly related to the blast wave energy. In this scenario, high-energy (GeV) radiation has been proposed to be a better proxy for the kinetic energy, since it is always deep in the fast cooling regime and it is less affected by IC losses (due to Klein-Nishina suppression). The tight correlation found between the luminosity of the temporally extended GeV emission and $E_{\gamma,\rm iso}$(Nava et al. 2014) supports this scenario. If this is the case, however, a question immediately arises: how can there be a correlation between L_X and $E_{\gamma,\rm iso}$ if the X-ray luminosity is not a proxy for the blast wave energy content $E_{\rm kin}$?

Both slow cooling and significant IC losses arise in low magnetic field regions, i.e. for small values of the magnetic equipartition parameter, $\epsilon_B \lesssim 10^{-2}$. Such small values are required for GeV-detected bursts if this emission arises from external shocks (Kumar & Barniol Duran 2009, 2010; Lemoine et al. 2013; Beniamini et al. 2015). Moreover, several recent studies not based on GRBs detected at GeV energies have found similar results, with an inferred ϵ_B distribution that peaks around 10^{-4} and extends down to $10^{-6}-10^{-7}$ (Barniol Duran 2014; Santana et al. 2014; Zhang et al. 2015; Wang et al. 2015). A theoretical explanation for such small values in the context of a decaying turbulence has been provided by Lemoine et al. (2013) and Lemoine et al. (2013b). These recent findings suggest another urgent question: how do the estimates of the kinetic energies (and in turn the estimates of the prompt efficiencies) change if the assumption on the typical values of ϵ_B in the range $0.1-0.01$ are modified, and more precisely, if smaller values are considered.

In this paper we address these two main issues. We explore whether the observed correlation between X-ray luminosities and prompt energetics implies that L_X is a proxy for the blast wave energy and can be used as a tool to derive the prompt efficiency. We then examine how are the estimates of these two quantities affected by different choices of ϵ_B. We proceed as follows. First we characterize the observed correlation using a sample of Swift GRBs (section 2). Then we consider the standard synchrotron/synchrotron self-Compton (SSC) afterglow model and derive (for different assumptions on the typical values and distributions of all the free parameters) the expected $L_X - E_{\gamma,\rm iso}$ correlation and compare it with the observations. For those sets of parameters for which the slope, normalization, and scatter of the observed correlation are reproduced, we check what is the cooling regime of the electrons emitting X-rays, and the relevance of their SSC losses. We find that the observed correlation can be reproduced also when SSC cooling is not negligible. To understand the origin of this result we present both simplified analytic estimates (section 3) and detailed numerical results (section 4). We also use the simulated X-ray luminosities to derive the blast wave kinetic energies and prompt efficiencies under the assumption of fast cooling and negligible IC cooling, as usually done with real X-ray observations. We compare these derived quantities with the simulated ones, to infer by how much the derived values differ from the simulated ones. The conclusions are discussed and summarized in section 5.

2 OBSERVATIONS

In order to compare the results of our simulations with observations we need to select a sample of GRBs with measured L_X and $E_{\gamma,\rm iso}$. We use the so-called BAT6 sample, a sample of long Swift GRBs carefully selected to be almost complete in redshift (for details see Salvaterra et al. 2012). The necessary information is available for 43 events. For this sample, the correlations $L_X - E_{\gamma,\rm iso}$ (for four different choices of the rest frame time at which L_X is computed) are presented in D'Avanzo et al. (2012). In the following we consider L_X at 11 hours: this is the most common value used in this and other correlation studies and it allows us a comparison of results derived using different samples. For the BAT6 sample, the values of L_X (integrated in the rest frame energy range 2-10 keV) can be found in Table 1 of D'Avanzo et al. (2012), while the values of the prompt en-

ergy $E_{\gamma,\rm iso}$ are reported in Nava et al. (2012). The resulting correlation is shown in Fig. 1. The best linear fit between L_X and $E_{\gamma,\rm iso}$ is given by:

$$L_{X,45} = 0.42\, E_{\gamma,\rm iso,52} \quad \text{with} \quad \sigma_{\log(\rm L_X/E_{\gamma,iso})} = 0.64 \qquad (1)$$

where $\sigma_{log(L_X/E_{\gamma,\rm iso})}$ is the 1σ scatter (measured in log-log space) [1]. The correlation between L_X at 11 hours and $E_{\gamma,\rm iso}$ has been investigated by different authors using different samples (see Nysewander et al. 2009, Margutti et al. 2013, and Wygoda et al. 2015 for recent investigations). These studies find statistically significant correlations between L_X and $E_{\gamma,\rm iso}$. The slope, normalization and scatter of the correlations discussed in these other studies are consistent with the one found in the BAT6 sample. Based on these findings, it has been argued that L_X must be a good proxy for the kinetic blast wave energy $E_{\rm kin}$.

3 ANALYTIC ESTIMATES

According to the standard forward shock afterglow theory if the X-ray emitting electrons are fast cooling then the X-ray luminosity, L_X is tightly related to the kinetic energy in the blast wave as $E_{\rm kin}/(1+Y)$, where Y is the Compton parameter. Previous studies (e.g. Kumar 2000; Freedman & Waxman 2001; Berger et al. 2003; Lloyd-Ronning & Zhang 2004; Berger 2007; Nysewander et al. 2009; D'Avanzo et al. 2012; Wygoda et al. 2015) assumed that Compton losses are small and neglected the factor $1+Y$. These estimates obtained low values of $E_{\rm kin}$ and hence implied puzzling large values of the prompt efficiency ϵ_γ. As $E_{\rm kin}$ is related to $E_{\gamma,\rm iso}$ the observed correlation between L_X and $E_{\gamma,\rm iso}$ has been interpreted as supporting the validity of the overall analysis and in particular the assumption of negligible Compton losses. We show here that the correlation persists even when Compton losses are important and $Y \gg 1$. In this case the inffered prompt efficiencies are much lower.

We begin by considering, once more, the model with no IC losses. In this case the X-ray luminosity (integrated in the rest frame energy range 2-10 keV), is given by:

$$L_{X,45} = \begin{cases} 1.6\ f(p) \left(\frac{1+z}{2}\right)^{\frac{2+p}{4}} \bar{\epsilon}_{e,-1}^{\,p-1}\ \epsilon_{B,-4}^{\frac{p-2}{4}} \\ \quad E_{\gamma,\rm iso,52}^{\frac{2+p}{4}} \left(\frac{1-\epsilon_\gamma}{\epsilon_\gamma}\right)^{\frac{2+p}{4}} t_{\rm 11hours}^{\frac{2-3p}{4}} \quad \text{for ISM} \\ \\ 1.7\ g(p) \left(\frac{1+z}{2}\right)^{\frac{2+p}{4}} \bar{\epsilon}_{e,-1}^{\,p-1}\ \epsilon_{B,-4}^{\frac{p-2}{4}} \\ \quad E_{\gamma,\rm iso,52}^{\frac{2+p}{4}} \left(\frac{1-\epsilon_\gamma}{\epsilon_\gamma}\right)^{\frac{2+p}{4}} t_{\rm 11hours}^{\frac{2-3p}{4}} \quad \text{for wind} \end{cases} \qquad (2)$$

where p is the power-law index of the electrons' energy spectrum, $f(p)$ and $g(p)$ are dimensionless functions of order unity defined such that $f(p=2.2) = g(p=2.2) = 1$, ϵ_e is the fraction of shock dissipated energy gained by electrons ($\bar{\epsilon}_e \equiv \epsilon_e(p-2)/(p-1)$), $t_{\rm 11hours}$ is the time since burst and z is the cosmological redshift. For typical values of p, Eq. 2 can be approximated by $L_{X,45}(11\,{\rm h}) \approx 2 \times \epsilon_{\rm e,-1} {\rm E_{kin,52}} \approx 2\,\epsilon_{\rm e,-1}[(1-\epsilon_\gamma)/\epsilon_\gamma]{\rm E_{\gamma,iso,52}}$, leaving out here a weak extra dependence on ϵ_B.

Eq. 2 has been traditionally used to infer $E_{\rm kin}$ from L_X. A comparison of $E_{\rm kin}$ with $E_{\gamma,\rm iso}$ can be used to estimate the prompt efficiency. The observed normalization of the $L_X - E_{\gamma,\rm iso}$ correlation (see Eq. 1) implied a large average efficiency, $\epsilon_\gamma \approx 0.8$. According to Eq. 2, $[L_{X,45}/E_{\gamma,\rm iso,52}]_{\rm no\ IC} \propto \epsilon_e \epsilon_\gamma^{-1}$. To account for the observed correlation the dispersion in both ϵ_γ and ϵ_e must be relatively small. As one is a prompt quantity while the other is an afterglow quantity, there is no a priori reason to expect the two to be correlated. The observed spread in the correlation (see Fig. 1) limits, therefore, the variability of each one of those quantities to about 1 dex (see a discussion in Nava et al. 2014).

Although the assumption of negligible IC losses is unclear for the X-ray emitting electrons, it must hold for the GeV emitting electrons for which IC is deep in the Klein Nishina region (see Beniamini et al. 2015 for a discussion). If the GeV luminosity is indeed produced by synchrotron in the forward shock, it should then be correlated to $E_{\gamma,\rm iso}$ according to Eq. 2. A correlation consistent with this scenario (but at an earlier observed time) has been indeed found by Nava et al. (2014).

We take now into account IC losses by the X-ray emitting electrons. We assume in this section that the IC cooling is in the Thomson regime and using the synchrotron forward shock model we estimate the X-ray afterglow luminosity L_X as a function of the afterglow free parameters. We assume that $\nu_m < \nu_c$ (where ν_m is the synchrotron frequencies), and $2 < p < 3$. The Compton parameter Y is given by (Sari & Esin 2001):

$$Y = \frac{\epsilon_e}{\epsilon_B(3-p)(1+Y)} \left(\frac{\nu_m}{\nu_c}\right)^{\frac{p-2}{2}}. \qquad (3)$$

Since we are interested in the situation where IC cooling is important, we explore the behaviour for $Y \gg 1$ (in our numerical estimates we will not be limited to this regime). In this limit:

$$Y \approx \begin{cases} 21\ \hat{f}(p)\ E_{\rm kin,53}^{\frac{p-2}{2(4-p)}}\ n_0^{\frac{p-2}{2(4-p)}}\ \epsilon_{B,-4}^{\frac{p-3}{4-p}} \times \\ \times \epsilon_{e,-1}^{\frac{p-1}{4-p}}\ t_{\rm 11hours}^{\frac{2-p}{2(4-p)}} \left(\frac{1+z}{2}\right)^{\frac{p-2}{2(4-p)}} \quad \text{ISM} \\ \\ 25\ \hat{g}(p)\, A_*^{\frac{p-2}{4-p}}\ \epsilon_{B,-4}^{\frac{p-3}{4-p}}\ \epsilon_{e,-1}^{\frac{p-1}{4-p}}\ t_{\rm 11hours}^{\frac{2-p}{4-p}} \left(\frac{1+z}{2}\right)^{\frac{p-2}{4-p}} \quad \text{Wind} \end{cases} \qquad (4)$$

where $\hat{f}(p)$ and $\hat{g}(p)$ are dimensionless functions of order unity defined such that $f(p=2.2) = g(p=2.2) = 1$, n_0 is the particle density in ${\rm cm}^{-3}$ and $A_* \equiv A/(5\times10^{11}{\rm g/cm})$ is the wind parameter. We have normalized $\epsilon_e, \epsilon_B, n_0, A_*$ to the values implied by recent literature (Kumar & Barniol Duran 2009, 2010; Lemoine et al. 2013; Barniol Duran 2014; Santana et al. 2014; Zhang et al. 2015; Wang et al. 2015).

In the regime $Y \gg 1$, at a given fixed time, Y depends very weakly on the unknown kinetic energy and density (see Eq. 4), and somewhat more strongly on the fraction of energy stored in the electrons and magnetic field:

- $Y \propto E_{\rm kin}^{1/18} n^{1/18} \epsilon_B^{-4/9} \epsilon_e^{2/3}$ for $p = 2.2$ and ISM medium
- $Y \propto E_{\rm kin}^{1/6} n^{1/6} \epsilon_B^{-1/3} \epsilon_e$ for $p = 2.5$ and ISM medium

[1] We use here and elsewhere in the text the notation $Q_x = Q/10^x$ in c.g.s. units as well as base 10 logarithms.

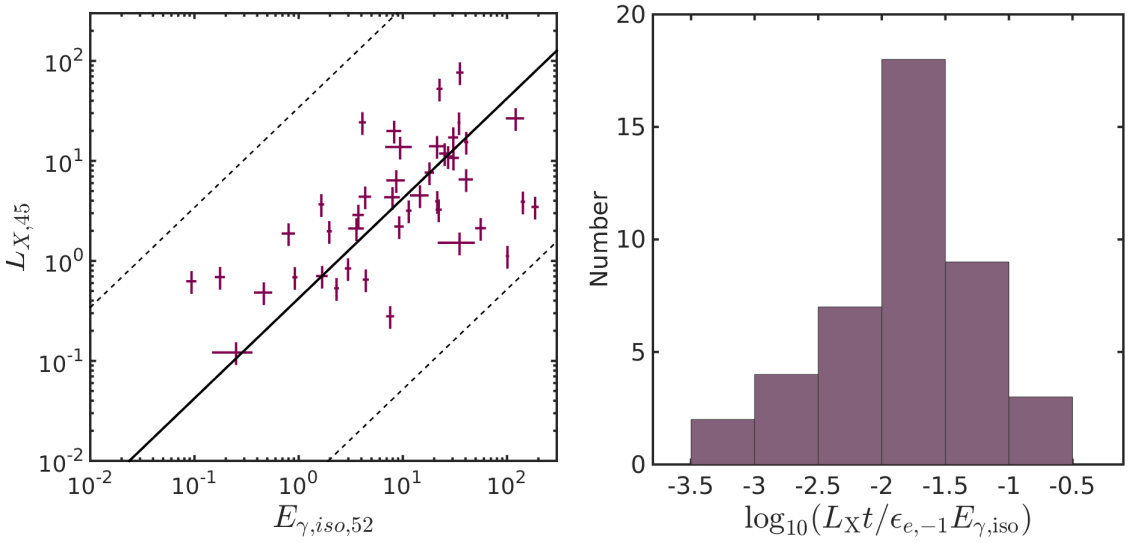

Figure 1. Correlation between the afterglow X-ray luminosity L_X and the prompt energy $E_{\gamma,\rm iso}$ for the sample of bursts presented in D'Avanzo et al. (2012). L_X is measured 11 hours after the burst trigger, integrated in the energy range 2-10 keV. In the left panel, the solid line depicts the best linear fit, corresponding to $L_{X,45} = 0.42\ E_{\gamma,\rm iso,52}$, while dashed lines show the 3σ scatter. In the right panel, following Nakar (2007), we plot a histogram of $L_X t/(\epsilon_{e,-1}E_{\gamma,\rm iso})$. If the X-ray flux is produced by synchrotron from fast cooling electrons with negligible IC, and the fraction of energy stored in the electrons is $\epsilon_e \approx 0.1$, this ratio would provide an estimate for $E_{\rm kin}/E_{\gamma,\rm iso}$).

- $Y \propto A_*^{1/9}\epsilon_B^{-4/9}\epsilon_e^{2/3}$ for $p = 2.2$ and wind medium
- $Y \propto A_*^{1/3}\epsilon_B^{-1/3}\epsilon_e$ for $p = 2.5$ and wind medium.

At this stage we already see that the dispersion that would be introduced due to the Y parameter is relatively small. The implied dispersion will become even weaker when we go back to L_X.

To determine the X-ray luminosity, one has first to determine the cooling regime of the X-ray producing electrons, i.e. the location of the cooling frequency ν_c as compared to the X-ray frequency ν_x. Following Granot & Sari (2002) and introducing a multiplicative factor of $(1+Y)^{-2}$ to account for IC cooling, we obtain (as long as $Y \gg 1$):

$$\nu_c \approx \begin{cases} 6.3\times10^{15}\ \tilde{f}(p)\ E_{\rm kin,53}^{\frac{-p}{2(4-p)}}\ n_0^{\frac{-2}{4-p}}\ \epsilon_{B,-4}^{\frac{-p}{2(4-p)}}\times \\ \times\epsilon_{e,-1}^{\frac{-2(p-1)}{4-p}}\ t_{\rm 11hours}^{\frac{3p-8}{2(4-p)}}\left(\frac{1+z}{2}\right)^{\frac{-p}{2(4-p)}}\ \text{Hz} \quad \text{ISM} \\ \\ 1.7\times10^{14}\ \tilde{g}(p)\ E_{\rm kin,53}^{\frac{1}{2}}\ A_*^{\frac{-4}{4-p}}\ \epsilon_{B,-4}^{\frac{-p}{2(4-p)}}\times \\ \times\epsilon_{e,-1}^{\frac{-2(p-1)}{4-p}}\ t_{\rm 11hours}^{\frac{3p-4}{2(4-p)}}\left(\frac{1+z}{2}\right)^{\frac{-(4+p)}{2(4-p)}}\ \text{Hz} \quad \text{Wind} \end{cases} \tag{5}$$

where $\tilde{f}(p), \tilde{g}(p)$ are dimensionless functions such that $\tilde{f}(p = 2.2) = \tilde{g}(p = 2.2) = 1$. According to these simple estimates, at ~ 11 hours, unless both ϵ_B and n are very small $\nu_c < \nu_x$, i.e. X-ray radiation at this time is typically emitted by "fast cooling" electrons. The first condition for using X-ray luminosities as a tool to derive $E_{\rm kin}$ appears then to be satisfied in most cases. It still remains to be seen whether the $L_X - E_{\gamma,\rm iso}$ correlation is expected in the regime $Y \gg 1$ (where the flux above ν_c is significantly suppressed by SSC cooling) and under what conditions it matches the observed one.

To derive L_X we divide the expression for the specific flux at frequencies larger than ν_c (Granot & Sari 2002) by a factor $(1+Y)$. We then integrate the specific flux between 2 keV and 10 keV to get the luminosity. We obtain:

$$\frac{L_{X,45}}{E_{\gamma,\rm iso,52}} = \begin{cases} 0.84\ \bar{f}(p)\ \epsilon_{\gamma,-1}^{\frac{(p-2)^2}{4(4-p)}-1}E_{\gamma,\rm iso,52}^{\frac{-(p-2)^2}{4(4-p)}}\ n_0^{\frac{2-p}{2(4-p)}}\ \epsilon_{B,-4}^{\frac{-(p^2-2p-4)}{4(4-p)}} \\ \times\epsilon_{e,-1}^{\frac{(p-1)(3-p)}{4-p}}\ t_{\rm 11hours}^{\frac{3p^2-12p+4}{4(4-p)}}\left(\frac{1+z}{2}\right)^{\frac{-(p^2-12)}{4(4-p)}} \quad \text{for ISM} \\ \\ 0.74\ \bar{g}(p)\ \epsilon_{\gamma,-1}^{\frac{2-p}{4}-1}E_{\gamma,\rm iso,52}^{\frac{p-2}{4}}\ A_*^{\frac{2-p}{4-p}}\ \epsilon_{B,-4}^{\frac{-(p^2-2p-4)}{4(4-p)}} \\ \times\epsilon_{e,-1}^{\frac{(p-1)(3-p)}{4-p}}\ t_{\rm 11hours}^{\frac{p(3p-10)}{4(4-p)}}\left(\frac{1+z}{2}\right)^{\frac{-(p^2+2p-16)}{4(4-p)}} \quad \text{for Wind} \end{cases} \tag{6}$$

where $\bar{f}(p), \bar{g}(p)$ are dimensionless functions such that $\bar{f}(p = 2.2) = \bar{g}(p = 2.2) = 1$.

The relation between L_X and $E_{\gamma,\rm iso}$ is almost linear, as the ratio $L_X/E_{\gamma,\rm iso}$ depends only weakly on $E_{\gamma,\rm iso}$: $L_X/E_{\gamma,\rm iso} \propto E_{\gamma,\rm iso}^{-0.018}$ for $p = 2.2$ in an ISM medium ($L_X/E_{\gamma,\rm iso} \propto E_{\gamma,\rm iso}^{0.05}$ for wind) and $L_X/E_{\gamma,\rm iso} \propto E_{\gamma,\rm iso}^{-0.09}$ for $p = 2.5$ in an ISM medium ($L_X/E_{\gamma,\rm iso} \propto E_{\gamma,\rm iso}^{0.125}$ for wind).

The ratio $L_{X,45}/E_{\gamma,\rm iso,52}$ depends very weakly on the density, and approximately scales as: $[L_{X,45}/E_{\gamma,\rm iso,52}]_{\rm with\ IC} \propto \epsilon_B^{1/2}\epsilon_e^{1/2}\epsilon_\gamma^{-1}$. This results should be compared with the situation of fast cooling without IC suppression: $[L_{X,45}/E_{\gamma,\rm iso,52}]_{\rm no\ IC} \propto \epsilon_e\epsilon_\gamma^{-1}$. The scaling in ϵ_γ is the same. Clearly, no correlation will appear in either case if the prompt efficiency varied significantly from one burst to another. When IC losses are negligible, the scatter of the correlation is related to the scatter of the parameters by $\sigma^2_{Log(L_X/E_{\gamma,\rm iso})} = \sigma^2_{\log\epsilon_e} + \sigma^2_{\log\epsilon_\gamma}$, where, following the reasoning at the top of the section, we have assumed that ϵ_e and ϵ_γ are independent. With significant IC cooling $\sigma^2_{Log(L_X/E_{\gamma,\rm iso})} = 0.25\sigma^2_{\log\epsilon_e} + 0.25\sigma^2_{\log\epsilon_B} + 0.5\sigma_{\log\epsilon_e\epsilon_B} + \sigma^2_{\log\epsilon_\gamma}$, where $\sigma_{\log\epsilon_e\epsilon_B}$ is the correlation coefficient between $\log_{10}(\epsilon_e)$ and $\log_{10}(\epsilon_B)$. Depending on the conditions determined by the forward shock, $\sigma_{\log\epsilon_e\epsilon_B}$ may be either positive or negative.

The additional scatter due to the new parameter ϵ_B is compensated by a weaker dependence on ϵ_e. Since both are microphysical parameters of the afterglow shock a possible anti correlation between the two can even reduce the overall scatter.

Keeping ϵ_e fixed, we note that the observed value 0.42 of the normalisation (see Eq. 1) can be reproduced by playing with the values of ϵ_B and ϵ_γ: a reasonable efficiency ($\epsilon_\gamma \approx 0.15$) is recovered for $\epsilon_B = 10^{-4}$, while higher values of ϵ_B require higher values of ϵ_γ (as ϵ_B increases, the assumption $Y \gg 1$ breaks down and we cannot use the equations derived in this section any more). We demonstrated that even for $Y \gg 1$ a correlation with the correct slope and normalization is expected.

Large Y might imply a bright SSC component at GeV energies, detectable with the Fermi/LAT. At $\sim$ 11 hours, under the most conservative assumption that the entire energy stored in the electrons is emitted as IC radiation we estimate a SSC flux $\sim 2 \times 10^{-12} E_{\rm kin,53} \epsilon_{e,-1} t_{11\rm hours}^{-1} d_{L28}^{-2}$ergs cm^{-2}sec^{-1}. This is orders of magnitude weaker than detectability limits with Fermi/LAT in the > 0.1 GeV range, which are typically 10^{-8}ergs cm^{-2}sec^{-1} (Ackermann et al. 2013a), and at best may approach 10^{-9}ergs cm^{-2}sec^{-1}, (see e.g. Ackermann et al. 2012). Moreover, the IC peak is expected to reside at energies > 10 GeV. This would reduce the prospects of detectability even further, since the LAT effective area quickly decreases at large energies. At earlier times ($t \sim 10 - 10^2$ seconds), and for the most energetic bursts (with $E_{\rm kin} \gtrsim 10^{54}$ergs) we can expect a total flux of $\sim 2 \times 10^{-8}$ergs cm^{-2}sec^{-1}. Even though marginally detectable, this SSC component might explain ($t \sim 10 - 10^2$ seconds) photons with energies that exceed the energy limit of synchrotron radiation (Wang et al. 2013; Tang et al. 2014).

4 NUMERICAL SIMULATIONS

Motivated by the approximate analytical scalings found in §3 we examine here numerically under which conditions the slope, normalization and scatter of the correlation can be reproduced. We consider synchrotron radiation from a forward shock afterglow, including IC corrections to the synchrotron spectrum. While in the previous section we discussed results in the two extreme regimes $Y \gg 1$ and $Y < 1$, here we solve numerically eq. 3, which is valid in both regimes. We find that the observed correlation is reproduced for a wide range of typical values and dispersions in the distributions of the afterglow parameters, also when SSC cooling is relevant.

We have calculated, first, for different values of ϵ_B and n what is the value of ϵ_γ needed in order to recover the normalization of the $L_X - E_{\gamma,\rm iso}$ correlation, for both ISM and wind external media. Fig. 2, depicts the results for $\epsilon_e = 0.1$ and $p = 2.2$ (the results depend only weakly on p). In both cases (ISM and wind) the resulting efficiency depends weakly on n (with an exception at low values of the wind parameter that we discuss later). The value of ϵ_γ depends strongly on the assumed value of ϵ_B: for large values of ϵ_B, SSC cooling is negligible, eq. 2 can be used, and a relatively large value of ϵ_γ is inferred. For smaller values of ϵ_B, larger kinetic energies are needed in the outflow and hence lower values of the efficiency are found. For relatively low values of the density and ϵ_B (low-left corner of the plane in Fig. 2), the X-ray emitting electrons are in the slow cooling regime (see Eq. 5). In this regime, only a fraction of the electrons' energy is actually emitted as radiation (be it synchrotron or IC). The required prompt efficiency ϵ_γ decreases as the density decreases, as more kinetic energy is needed in the outflow when the system gets deeper into the slow cooling regime.

The scatter of the $L_X - E_{\gamma,\rm iso}$ correlation depends on the width of the distributions of the parameters involved. The fact that a correlation is observed with a given dispersion limits the dispersion of such parameters. In order to estimate the widths of the relevant distributions we apply a Monte Carlo method: we assign a given distribution to each free parameter, randomly draw a value and using the forward shock afterglow synchrotron + IC model we calculate L_X for each realization. We draw 10^5 realizations and compare the obtained correlation with the observed one and derive the conditions required to reproduce the observations.

For two of the parameters ($E_{\gamma,\rm iso}$ and z) the distributions are deduced from observations. In order to compare the simulated correlation with the observed correlation in the D'Avanzo et al. (2012) BAT6 sample we use that sample to obtain the distributions of $E_{\gamma,\rm iso}$ and z. The distribution of $E_{\gamma,\rm iso}$ is taken from observations of bursts with known redshift. Using D'Avanzo et al. (2012) we consider a log-normal distribution with a mean value: $\langle E_{\gamma,\rm iso} \rangle = 8 \times 10^{52}$ergs and a standard deviation $\sigma_{log E_{\gamma,\rm iso}} = 0.75$. For redshifts, we fit the distribution of bursts used by D'Avanzo et al. (2012) and take a log-normal distribution with a peak at $z = 1$ and a standard deviation of 0.3 dex. For the other parameters we consider lognormal distributions for ϵ_B, n (or A_*), and ϵ_e, and either a fixed value or a uniform distribution for p. For ϵ_e we choose $\langle \log_{10}(\epsilon_e) \rangle = -1$ and $\sigma_{log\epsilon_e} = 0.3$ in all the simulations: ϵ_e is indeed confined both from observations (Santana et al. 2014; Nava et al. 2014) and from numerical simulations (Sironi & Spitkovsky 2011) to have a narrow distribution peaked around $\epsilon_e = 0.1$ (see Beniamini et al. 2015 for a detailed discussion). For ϵ_B and n we test different average values and widths. The intrinsic distributions of these parameters are less certain. However, typical values for the 1 σ dispersion found for both these parameters in GRB modelling are of order 1 dex (Santana et al. 2014; Zhang et al. 2015). Therefore, these are the canonical values that we consider here. Since Soderberg et al. (2006) find a somewhat wider distribution for n (consistent with $\sigma = 1.7$ dex), we explore also the possibility of wider density distributions ($\sigma = 1.5, 2$ dex). Since L_X depends very weakly on n, its dispersion can be significantly increased with minor effects to the overall results. Finally, ϵ_γ and its scatter are chosen such that the normalization and scatter of the $L_X - E_{\gamma,\rm iso}$ correlation are reproduced (see Eq. 1). Considering the detectability limits of Swift/XRT (Gehrels et al. 2004), we apply a lower limit on the X-ray flux of $\sim 2 \times 10^{-14}$ergs cm^{-2}s^{-1}.

A summary of different input parameters for which $\sigma_{log\epsilon_B}, \sigma_{logn} \geqslant 1$ and for which observations are satisfactorily reproduced is reported in Table 1. This is of course not an exhaustive list, as the correlation could also be reproduced with a smaller scatter in ϵ_B, n by considering a larger scatter in $\epsilon_\gamma, \epsilon_e$. As long as the dispersion in the intrinsic parameters satisfies $\sigma_{log\epsilon_B}, \sigma_{logn} \leqslant 1.2$ (or for instance

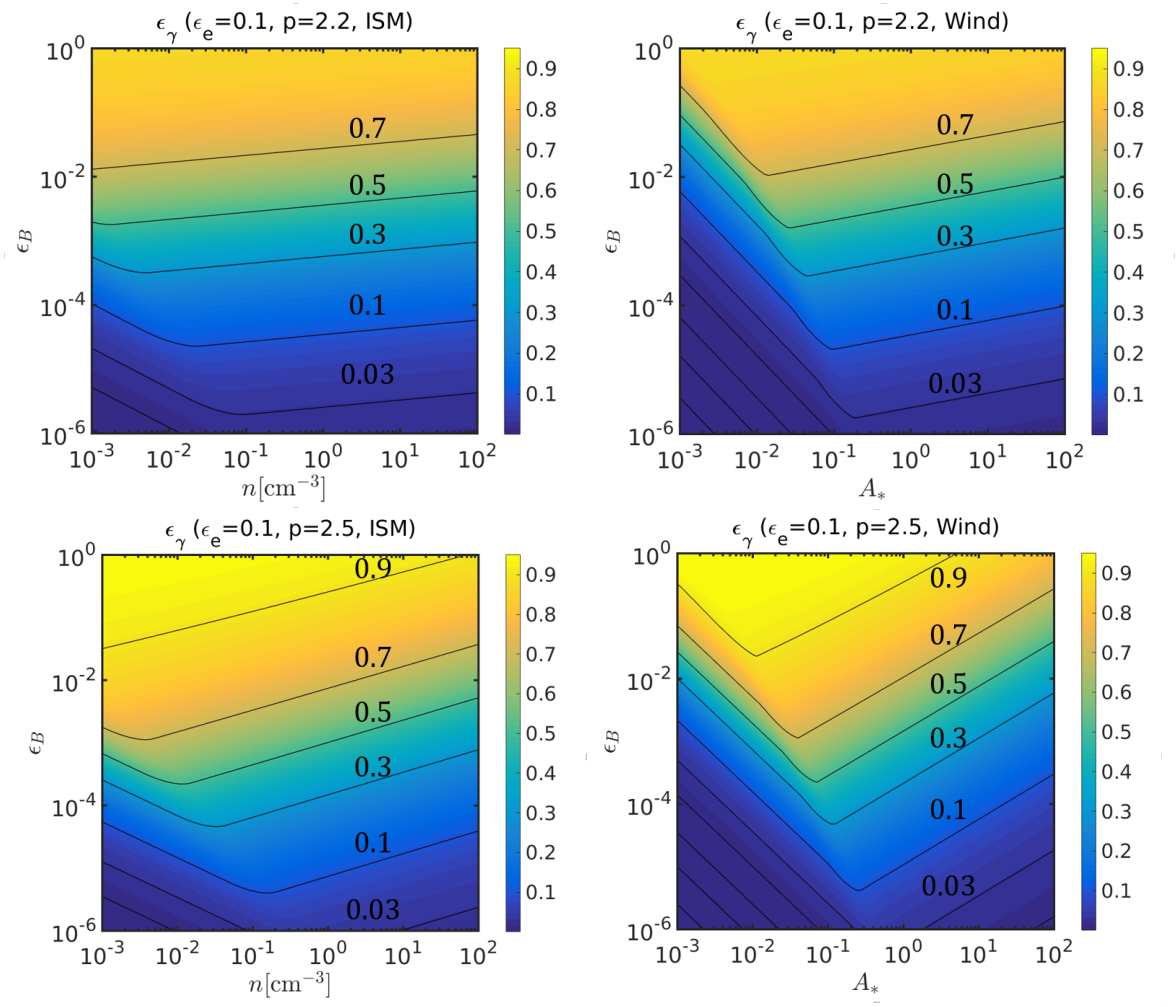

Figure 2. ϵ_γ implied by the normalization of the observed $L_X - E_{\gamma,\rm iso}$ correlation as a function of the density and ϵ_B for $\epsilon_e = 0.1$ (left panels: ISM; right panels: wind; top panels: $p = 2.2$; bottom panels: $p = 2.5$).

$\sigma_{log\epsilon_B} \leqslant 1$, $\sigma_{logn} \leqslant 2$), the correlation in the $L_X - E_{\gamma,\rm iso}$ plane is recovered. For each of the realizations, we also estimate, from the calculated X-ray luminosities and the input $E_{\gamma,\rm iso}$, the kinetic energy $E_{\rm kin,2}$ and efficiency $\epsilon_{\gamma,2}$ that would have been derived using eq. 2, namely, assuming fast cooling and neglecting SSC. We perform these estimates for an ISM medium, $\epsilon_e = 0.1, \epsilon_B = 0.01, n = 1\mathrm{cm}^{-3}$ and $p = 2.2$ for all bursts. Table 1 summarizes $\epsilon_{\gamma,2}$, the ratio $E_{\rm kin,2}/E_{\rm kin,real}$ and the percentage of simulated GRBs for which $\nu_x > \nu_c$. The results depend strongly on the assumed average value of ϵ_B, and they depend very weakly on the mean value of n, on the nature of the external medium and on the value of p (see Table 1). As expected, for low values of ϵ_B the values of the kinetic energy and efficiency derived assuming $Y \lesssim 1$ and fast cooling deviate significantly from those used for the simulations. Eq. 2 fails to recover the true (i.e. simulated) values of the parameters, smaller kinetic energies are inferred and consequently, larger prompt efficiencies.

Since the main parameter determining the results is ϵ_B, in Fig. 3 we show the resulting $L_X - E_{\gamma,\rm iso}$ correlation for 43 simulated bursts (so as to fit the number of bursts in the BAT6 sample) for three cases: $\langle \log_{10} \epsilon_B \rangle = -2$ (upper left panel), $\langle \log_{10} \epsilon_B \rangle = -4$ (middle left panel) and $\langle \log_{10} \epsilon_B \rangle = -6$ (lower left panel). For each simulation, Fig. 3 also shows the ratio between the kinetic energies inferred using eq. 2 and the simulated one (panels on the right). For $\langle \log_{10} \epsilon_B \rangle = -4$ ($\langle \log_{10} \epsilon_B \rangle = -2$), we get $E_{\rm kin,2}/E_{\rm kin,real} = 0.04^{+0.08}_{-0.03}$ ($E_{\rm kin,2}/E_{\rm kin,real} = 0.28^{+0.45}_{-0.17}$). Naturally, this affects also the estimates of the prompt efficiencies. In Fig. 4 we explicitly show how the ratio of the derived to real efficiency varies as a function of the mean value of ϵ_B for both ISM and wind environments. In both cases $\epsilon_B \lesssim 10^{-3}$ leads to a significant deviation (of order $\gtrsim 2$) of the derived efficiency as compared with the real one.

5 DISCUSSION AND CONCLUSIONS

The kinetic energy of the blast wave (during the afterglow phase) and the corresponding efficiency of the prompt phase are among the most important parameters concerning the emission regions in GRBs. Following Kumar (2000) and Freedman & Waxman (2001) the X-ray luminosity at 11 hours has been traditionally used to infer the kinetic energy (Berger et al. 2003; Lloyd-Ronning & Zhang 2004;

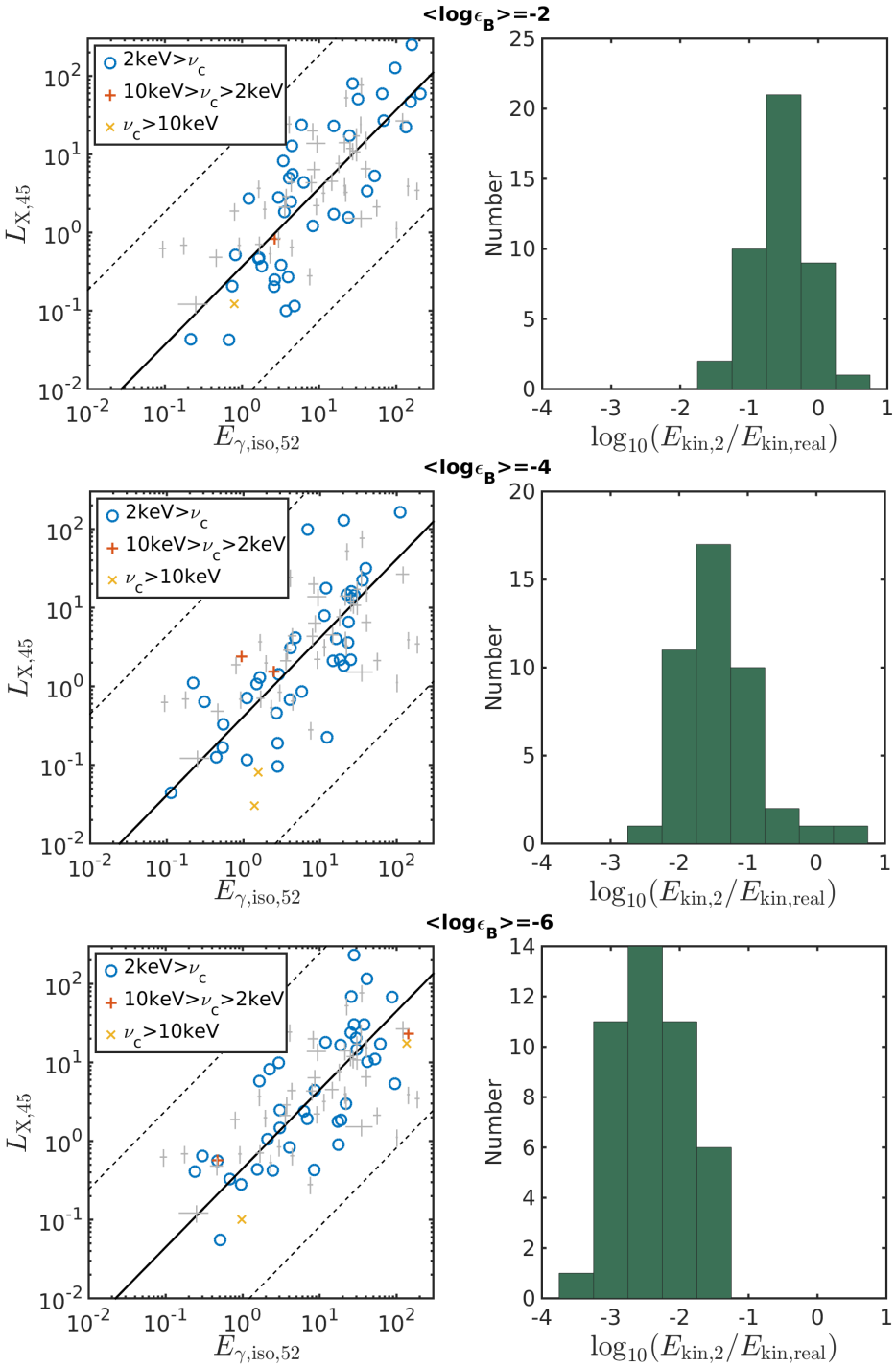

Figure 3. Results of MC simulations for different assumptions on the median value of the magnetic field: $\epsilon_B = 10^{-2}$ (upper panels), $\epsilon_B = 10^{-4}$ (middle panels), $\epsilon_B = 10^{-6}$ (lower panels). All the other parameters are the same in the three different simulations: $\sigma_{log\epsilon_B} = 1$, an ISM medium with $\langle \log_{10}(n[\mathrm{cm}^{-3}]) \rangle = 0, \sigma_{logn} = 1$, a log-normal distribution of ϵ_e with $\langle \log_{10}(\epsilon_e) \rangle = -1, \sigma_{log\epsilon_e} = 0.3$, $p = 2.2$, and a redshift distribution which is log-normal with a peak at $z = 1$ and a standard deviation of 0.3 dex. ϵ_γ is chosen such that the normalization of the observed $L_X - E_{\gamma,\mathrm{iso}}$ correlation is reproduced (see Fig. 2). For each simulation, the left panel shows the simulated $E_{\gamma,\mathrm{iso}} - L_X$ relation for 43 randomly selected bursts (circles denote bursts with $\nu_c < 2$keV, pluses, bursts with $2\,\mathrm{keV} < \nu_c < 10\,\mathrm{keV}$ and X's, bursts with $\nu_c > 10\,\mathrm{keV}$). Grey crosses refer instead to the 43 GRBs in the sample of D'Avanzo et al. 2012 (see also Fig. 1). Solid lines depict the best linear fits and dashed lines depict the 3σ scatter of the simulated correlation. The panel on the right shows the ratio between the kinetic energies derived using Eq. 2 and the simulated (see text for details).

	Simulations' input parameters				Results			
varying parameter	Medium	p	$\log_{10}(\epsilon_B)$ $\pm\sigma_{\log_{10}(\epsilon_B)}$	$\log_{10}(n)$ $\log_{10}(A_*)$	$\epsilon_{\gamma,\rm real}$	$\epsilon_{\gamma,2}$	$\frac{E_{\rm kin,2}}{E_{\rm kin,real}}$	% fast cooling
ϵ_B	ISM	2.2	-1 ± 1	0 ± 1	$0.78^{+0.22}_{-0.25}$	$0.75^{+0.25}_{-0.19}$	$0.52^{+0.65}_{-0.29}$	99
	ISM	2.2	-2 ± 1	0 ± 1	$0.61^{+0.31}_{-0.2}$	$0.76^{+0.24}_{-0.19}$	$0.28^{+0.45}_{-0.17}$	97
	ISM	2.2	-3 ± 1	0 ± 1	$0.36^{+0.2}_{-0.13}$	$0.75^{+0.25}_{-0.2}$	$0.11^{+0.23}_{-0.07}$	96
	ISM	2.2	-4 ± 1	0 ± 1	$0.16^{+0.12}_{-0.07}$	$0.74^{+0.29}_{-0.21}$	$0.04^{+0.08}_{-0.03}$	92
	ISM	2.2	-5 ± 1	0 ± 1	$0.06^{+0.05}_{-0.03}$	$0.74^{+0.26}_{-0.2}$	$0.01^{+0.028}_{-0.008}$	88
	ISM	2.2	-6 ± 1	0 ± 1	$0.02^{+0.02}_{-0.01}$	$0.73^{+0.27}_{-0.22}$	$0.004^{+0.009}_{-0.003}$	82
n	ISM	2.2	-4 ± 1	-1 ± 1	$0.17^{+0.09}_{-0.06}$	$0.75^{+0.27}_{-0.2}$	$0.04^{+0.09}_{-0.03}$	73
	ISM	2.2	-4 ± 1	1 ± 1	$0.14^{+0.12}_{-0.06}$	$0.74^{+0.26}_{-0.22}$	$0.03^{+0.07}_{-0.02}$	99
	ISM	2.2	-4 ± 1	0 ± 1.5	$0.16^{+0.09}_{-0.06}$	$0.75^{+0.25}_{-0.2}$	$0.03^{+0.07}_{-0.02}$	84
	ISM	2.2	-4 ± 1	0 ± 2	$0.16^{+0.08}_{-0.05}$	$0.76^{+0.24}_{-0.2}$	$0.03^{+0.08}_{-0.02}$	75
density profile	wind	2.2	-2 ± 1	0 ± 1	$0.61^{+0.25}_{-0.18}$	$0.8^{+0.2}_{-0.18}$	$0.24^{+0.41}_{-0.15}$	98
	wind	2.2	-4 ± 1	0 ± 1	$0.16^{+0.12}_{-0.07}$	$0.76^{+0.24}_{-0.21}$	$0.03^{+0.08}_{-0.02}$	89
p	ISM	[2.1-2.7]	-2 ± 1	0 ± 1	$0.61^{+0.31}_{-0.2}$	$0.87^{+0.13}_{-0.12}$	$0.15^{+0.3}_{-0.1}$	96
	ISM	[2.1-2.7]	-4 ± 1	0 ± 1	$0.16^{+0.12}_{-0.07}$	$0.82^{+0.18}_{-0.18}$	$0.02^{+0.05}_{-0.01}$	88
	ISM	2.5	-2 ± 1	0 ± 1	$0.72^{+0.28}_{-0.21}$	$0.91^{+0.09}_{-0.11}$	$0.11^{+0.2}_{-0.07}$	93
	ISM	2.5	-4 ± 1	0 ± 1	$0.26^{+0.18}_{-0.11}$	$0.92^{+0.08}_{-0.1}$	$0.02^{+0.04}_{-0.01}$	80
$\sigma_{\log\epsilon_B},\sigma_{\log n}$	ISM	2.2	-2 ± 1.2	0 ± 1.2	$0.61^{+0.19}_{-0.15}$	$0.8^{+0.2}_{-0.14}$	$0.25^{+0.49}_{-0.17}$	95
	ISM	2.2	-4 ± 1.2	0 ± 1.2	$0.16^{+0.04}_{-0.03}$	$0.73^{+0.27}_{-0.22}$	$0.04^{+0.1}_{-0.03}$	89

Table 1. List of the input parameters (on the left) and results (on the right) for different simulations. We fix all the afterglow parameters and vary one parameter at a time (as indicated in the first column). For the case of $p=[2.1-2.7]$, p is drawn from a uniform distribution between 2.1 and 2.7. For the results we report the allowed range (in order to fit the observed correlation and scatter) for the "real" prompt efficiency $\epsilon_{\gamma,real}$ (calculated using the simulated kinetic and γ-ray energies), the prompt efficiency $\epsilon_{\gamma,2}$ as inferred from the simulated luminosities applying eq. 2, the average ratio between the kinetic energy inferred from eq. 2 and the input kinetic energy $E_{\rm kin,real}$, and the fraction of simulated GRBs for which X-rays are emitted by electrons that are fast cooling. Reported errors are all at the 1σ level.

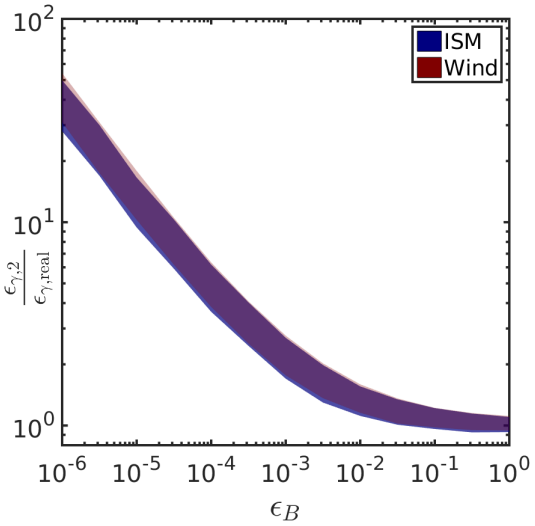

Figure 4. The ratio of the derived prompt γ-ray efficiency (assuming fast cooling synchrotron with no IC suppression) compared to the actual simulated efficiency as a function of ϵ_B for an ISM and a wind. In all simulations we use $\langle\log_{10}(n[\rm cm^{-3}])\rangle=0$ ($\langle\log_{10}(A_*)\rangle=0$), and standard deviations of 1dex in the density (or wind parameter) and ϵ_B and $p=2.2$.

Berger 2007; Nysewander et al. 2009; D'Avanzo et al. 2012; Wygoda et al. 2015) resulting usually in very large prompt efficiencies. This method has been claimed to be quite robust, since no other quantities apart from ϵ_e and ϵ_γ are involved. We have re-investigated the question whether the X-ray are indeed a good proxy for $E_{\rm kin}$. This is motivated by the recent findings that the typical values of ϵ_B might be much smaller than the values 0.01-0.1 traditionally assumed. An additional line of motivation is the apparent contradiction between energies estimated in this way using the X-ray flux as compared with the energies estimated using the 0.1-10 GeV radiation detected by Fermi/LAT (Beniamini et al. 2015). In that paper we have argued that this contradiction can be resolved within the synchrotron forward shock scenario if the X-ray emitting electrons are either slow cooling or else, they are strongly affected by IC cooling: in both cases, the X-ray emission is not a good proxy for the energy of the blast wave. These conclusions are however model dependent, since they rely on the assumption that the GeV radiation is synchrotron emission from the external shock. Other studies considered an alternative possibility, in which the GeV radiation is not of afterglow origin (e.g. Beloborodov 2014).

For $\epsilon_B \sim 0.01 - 0.1$ (and $\epsilon_e \sim 0.1$), SSC losses are small and the afterglow synchrotron luminosity above the characteristic synchrotron frequencies is proportional to ϵ_e times the kinetic energy of the blast wave $E_{\rm kin}$. The relation between the X-ray flux and the kinetic energy (eq. 2) depends very weakly on ϵ_B and is independent of the density. Thus, the observed correlation between L_X and $E_{\gamma,\rm iso}$ gave support to the fact that L_X can be used to infer $E_{\rm kin}$.

For smaller values of ϵ_B, SSC cannot be ignored and L_X depends indirectly on ϵ_B. This is the main parameter regulating the importance of SSC vs. synchrotron emission as well as determining whether X-ray emitting electrons are slow or fast cooling. We show here that somewhat surprisingly the observed $L_X - E_{\gamma,\rm iso}$ correlation is recovered also when the full effect of ϵ_B on L_X is taken into account. For small ϵ_B values, $L_{\rm GeV}$ (not affected by SSC cooling) rather than L_X, is a good proxy for the kinetic energy, and is indeed strongly correlated with $E_{\gamma,\rm iso}$ (Nava et al. 2014).

SSC cooling modifies the synchrotron spectrum so that the cooling frequency is $\nu_c = \nu_c^{syn}/(1+Y)^2$ and the luminosity above ν_c is $L(\nu > \nu_c) = L(\nu > \nu_c)^{syn}/(1+Y)$. By means of analytic and numerical estimates we found that the X-ray frequency most likely lies in this part of the synchrotron spectrum, even for small $\epsilon_B \sim 10^{-6}$. The observed L_X is then suppressed by a factor $(1+Y)$. This factor, $(1+Y)$, depends only weakly on the energy and the relation between L_X and $E_{\gamma,\rm iso}$ is still linear. This means that approximately $L_X/E_{\gamma,\rm iso} \propto \epsilon_e^{1/2}\epsilon_B^{1/2}\epsilon_\gamma^{-1}$ (with possibly a weak dependence on n for small n values), instead of $\propto \epsilon_e\epsilon_\gamma^{-1}$. While an additional parameter was added, the dependence on both it and ϵ_e is smaller than before, and hence it is reasonable to have a comparable spread. The observed correlation is reproduced under very reasonable assumptions (Table 1). The normalization and scatter of the correlation can be recovered even with very small values of $\epsilon_B \gtrsim 10^{-6}$, demonstrating that the recent findings of small magnetic field are not at odds with the existence of a clear trend between L_X and $E_{\gamma,\rm iso}$.

We reconfirm the results of our previous work (Beniamini et al. 2015), that generally, L_X is not a good proxy for the kinetic energy and that on its own the GeV afterglow luminosity, L_{GeV} is much better proxy for the blast wave kinetic energy. When both are combined, both this energy and ϵ_B can be determined. Including IC corrections to L_X, we find larger kinetic energies and lower efficiencies than reported in studies assuming no IC suppression. More specifically, lower values of the prompt efficiency ($\epsilon_\gamma \lesssim 0.2$), can be accounted for by invoking lower values of the magnetic field ($\epsilon_B \lesssim 10^{-4}$), while if larger values of ϵ_B are assumed, then larger values of the prompt efficiency must be invoked to match the observations. Estimates of the kinetic blast wave energies are fundamental not only to determine the energetics of the system, but also to infer the efficiency of the mechanism producing the prompt radiation (i.e. the ratio between the energy radiated in the prompt phase $E_{\gamma,\rm iso}$ and the initial outflow energy $E_{\gamma,\rm iso} + E_{\rm kin}$). In the past, the large inferred value of ϵ_γ has been claimed as one of the main arguments against the internal shock model, within which large efficiencies can hardly be achieved. In fact, obtaining order unity efficiencies is very problematic in a wide range of models, including most models invoking magnetic reconnection. Thus, reducing the requirements on the efficiency, opens up somewhat the parameter space of allowed prompt models and we may have to reconsider our picture of the prompt phase in light of these results.

We thank Rodolfo Barniol Duran and Pawan Kumar for helpful comments. We acknowledge support by the John Templeton Foundation, by a grant from the Israel Space Agency, by a ISF-CNSF grant and by the ISF-CHE I-core center for excellence for research in Astrophysics. LN was supported by a Marie Curie Intra-European Fellowship of the European Community's 7th Framework Programme (PIEF-GA-2013- 627715).

REFERENCES

Ackermann, M., et al., 2012, ApJ, 754,121.
Ackermann, M., Ajello, M., Asano, K., et al., 2013a, ApJS, 209, 11.
Barniol Duran, R., 2014, MNRAS, 442, 3147.
Beloborodov, A. M., 2000, Ap. J. Lett., 539, L25.
Beloborodov A. M., Hascöet R., Vurm I., 2014, ApJ, 788, 36.
Beniamini P., Piran T., 2013, ApJ, 769, 69.
Beniamini, P., & Granot, J., 2016, MNRAS, tmp, 692B (arXiv:1509.02192).
Beniamini, P., & Piran, T., 2014, MNRAS, 445, 3892B.
Beniamini, P., Nava, L., Barniol Duran, R., & Piran, T., 2015, MNRAS, 454, 1073B.
Berger, E., Kulkarni, S. R., & Frail, D. A. 2003, ApJ, 590, 379.
Berger, E. 2007,ApJ,670, 1254.
Bošnjak, Ž., Daigne, F., and Dubus, G. A&A 498, 677 (2009).
D'Avanzo, P., Salvaterra, R., Sbarufatti, B., et al. 2012, MNRAS, 425, 506.
Daigne, F., and R. Mochkovitch, 1998, Mon. Not. RAS 296, 275.
Daigne F., Bosnjak Z., Dubus G., 2011, A&A, 526, 110.
Derishev, E. V., Kocharovsky, V. V., Kocharovsky, V. V., 2001, A&A, 372, 10711077.

Freedman D. L., Waxman E., 2001, ApJ, 547, 922.
Gehrels N. et al., 2004, ApJ, 611, 1005.
Granot J., Sari R., 2002, ApJ, 568, 820.
Granot J., Königl A., Piran T., 2006, MNRAS, 370, 1946.
Granot J., Piran T., Bromberg O., et al. 2015, SSRv, 191, 471G.
Guetta, D., M. Spada, and E. Waxman, 2001, Ap. J., 557, 399.
Ioka, K., Toma, K., Yamazaki, R., & Nakamura, T. 2006, A&A,458, 7.
Kobayashi, S., T. Piran, and R. Sari, 1997, Ap. J., 490, 92+.
Kumar, P., 1999, ApJ 523, L113.
Kumar P., 2000, ApJ, 538, L125.
Kumar, P., & Barniol Duran, R. 2009, MNRAS 400, L75.
Kumar, P., & Barniol Duran, R. 2010, MNRAS 409, 226.
Kumar P., Crumley P., 2015, MNRAS, 453, 1820.
Lazzati D., Ghisellini G., Celotti A., 1999, MNRAS, 309, L13
Lemoine M., Li Z., Wang X.-Y., 2013, MNRAS, 435, 3009.
Lemoine M., 2013, MNRAS, 428, 845.
Lloyd-Ronning, N. M., & Zhang, B. 2004, ApJ, 613, 477.
Margutti, R., Zaninoni, E., Bernardini, M. G., et al., 2013, MNRAS 428, 729.
Nakar E., 2007, Phys. Rep., 442, 166.
Nava, L., Salvaterra, R., Ghirlanda, G., et al. 2012, MNRAS, 421, 1256.
Nava, L., Vianello G., Omodei N., et al., 2014, MNRAS, 443, 3578.
Nousek, J. A., Kouveliotou, C., Grupe, D., et al. 2006, ApJ, 642,389.
Nysewander, M., Fruchter, A. S., & Peer, A., 2009, ApJ, 701, 824.
Salvaterra R., Campana S., Vergani S. D., et al., 2012, ApJ, 749, 68.
Santana, R., Barniol Duran, R., Kumar, P., 2014, ApJ, 785, 29.
Sari R. & Esin A., 2001, ApJ, 548, 787.
Soderberg, A. M., Berger, E., Kasliwal, M., et al. 2006, ApJ, 650, 261.
Sironi, L., & Spitkovsky, A. 2011, ApJ, 726, 75.
Tang Q.-W., Tam, P., Wang, X.-Y., 2014ApJ, 788, 156.
Vurm, I., Lyubarski, Y., Piran, T., 2013, ApJ, 764, 143.
Wang, X.-Y., Liu, R-Y., Lemoine, M., 2013, ApJ, 771, 33.
Wang, X.-G., Zhang, B., Liang, E.-W., et al. 2015, arXiv:1503.03193.
Wygoda, N., Guetta, D., Mandich, M.-A., & Waxman, E. 2015, arXiv:1504.01056.
Zhang, B., Liang, E., Page, K. L., et al. 2007,ApJ,655, 989.
Zhang, B., & Yan, H. 2011, ApJ, 726, 90.
Zhang B.-B., van Eerten H., Burrows D. N., Ryan G. S., Racusin J. L., Troja E., MacFadyen A., 2015, ApJ, 806, 15.